Supporting Information:

Mechanistic insight into the non-hydrolytic *sol-gel* process of tellurite glass films to attain a high transmission

Xuanzhao Pan[1,5,6], Jiangbo Zhao[1,2,5]*, Gujie Qian[3,4], Xiaozhou Zhang[1,5,6], Yinlan Ruan[1,5], Andrew Abell[1,5,6], and Heike Ebendorff-Heidepriem[1,5]

[1] *Institute for Photonics and Advanced Sensing, University of Adelaide, Adelaide, SA 5005, Australia*
[2] *Leibniz Institute of Photonic Technology, Jena 07745, Germany*
[3] *Natural and Built Environments Research Centre, School of Natural and Built Environments, University of South Australia, Mawson Lakes, SA 5095, Australia*
[4] *College of Science and Engineering, Flinders University, Bedford Park, SA 5042, Australia*
[5] *ARC Centre of Excellence for Nanoscale BioPhotonics*
[6] *Department of Chemistry, School of Physical Sciences, The University of Adelaide, South Australia.*

*Correspondence and requests for materials should be addressed to J.Z. tim.zhao@adelaide.edu.au

Experimental section

Materials and sample preparations

Reagents: TeO_2 powder (TeO_2, Suzhou Sinosun, 99.999%), Zn-acetate di-hydrate crystals ($Zn(CH_3COO)_2{\cdot}2H_2O$, Sigma Aldrich, 99.0%), Na-acetate crystals (CH_3COONa, Sigma Aldrich, 99.0%), 1,2-propanediol solvent (Sigma Aldrich, 99.5%), and p-toluene sulfonic acid monohydrate crystals (PTSA, Sigma Aldrich, 98.5%) were used as received without purification or pre-treatment.

Preparation of Te-alkoxide ($Te(O_2C_3H_6)_2$): In brief, TeO_2 powder and PTSA crystals (as catalyst) were added into 1,2-propanediol in a 100-ml round bottom flask, with a molar ratio of 0.1:0.01:1. By heating the mixture at 150 °C under refluxing with moderate stirring (~1000 rpm) for about 6 h, a considerable amount of Te-alkoxide crystals was yielded with by-products. To extract high-purity Te-alkoxide molecules, the resulting mixture was processed *via* suction filtration. To enhance the extraction rate of Te-alkoxide crystals, we collected this filtration when the mixture was hot. Te-alkoxide crystals were then precipitated by retaining the filtrate in a refrigerator (at ~2 °C) for > 3 days, during which particulate-form Te-alkoxide was recrystallized from the saturated solution. Subsequently, high-quality Te-alkoxide crystlas were collected by centrifugation and vacuum-drying. This as-prepared Te-alkoxide was used as the precursor for synthesis of TZN *sol-gel* [1].

Preparation of TZN sol: Firstly, Te-alkoxide (1 M), Zn-acetate (1 M) and Na-acetate (1 M) solutions were prepared *via* dissolving the respective crystals in 1,2-propanediol under heating (~60 °C) and stirring (~1000 rpm) for about 30 mins in a round-bottom flask. These solutions were then mixed, with a molar ratio of Te:Zn:Na = 80:10:20, followed by heating at 80 °C for 2 h to form TZN *sol*. The *sol* was aged in a desiccator at room temperature for different days as summarized in Table 1. Prior to the film preparation, the TZN *sol* was centrifuged at 14800 rpm for 15 mins to remove any unwanted large particulates. Note refluxing was applied for steps with heating.

Preparation of TZN-based glass film in open air: The aged TZN *sol* was deposited onto a substrate by spin coating, e.g., 2000 rpm for 60 seconds with an acceleration of 100 rpm/s. The coated-substrates were subsequently heated (ramp up rate 5 °C/min) for 12-72 h at varying temperatures (72 h at 80 °C, 12 h at130 °C, and 12h at 150 °C) to acquire the TZN *xerogel* films, which were further processed at elevated temperatures (300 °C, 400 °C and 500 °C) with a heat up rate of 1 °C/min and dwell time of 1 h. With regard to the substrate used for film preparation, pre-cleaned Si wafers and glass coverslips were selected for μ-XRD analysis and optical characterizations, respectively.

Preparation of TZN-based xerogel powder in open air: The same aged TZN *sols* used for glass film production were placed in opened vials and heated for 12-72 h at different temperature (72 h at 80 °C, and 12 h at 130 °C, 150 °C or 160 °C). The collected TZN *xerogel* powders were used for color inspection and TG-DSC measurement.

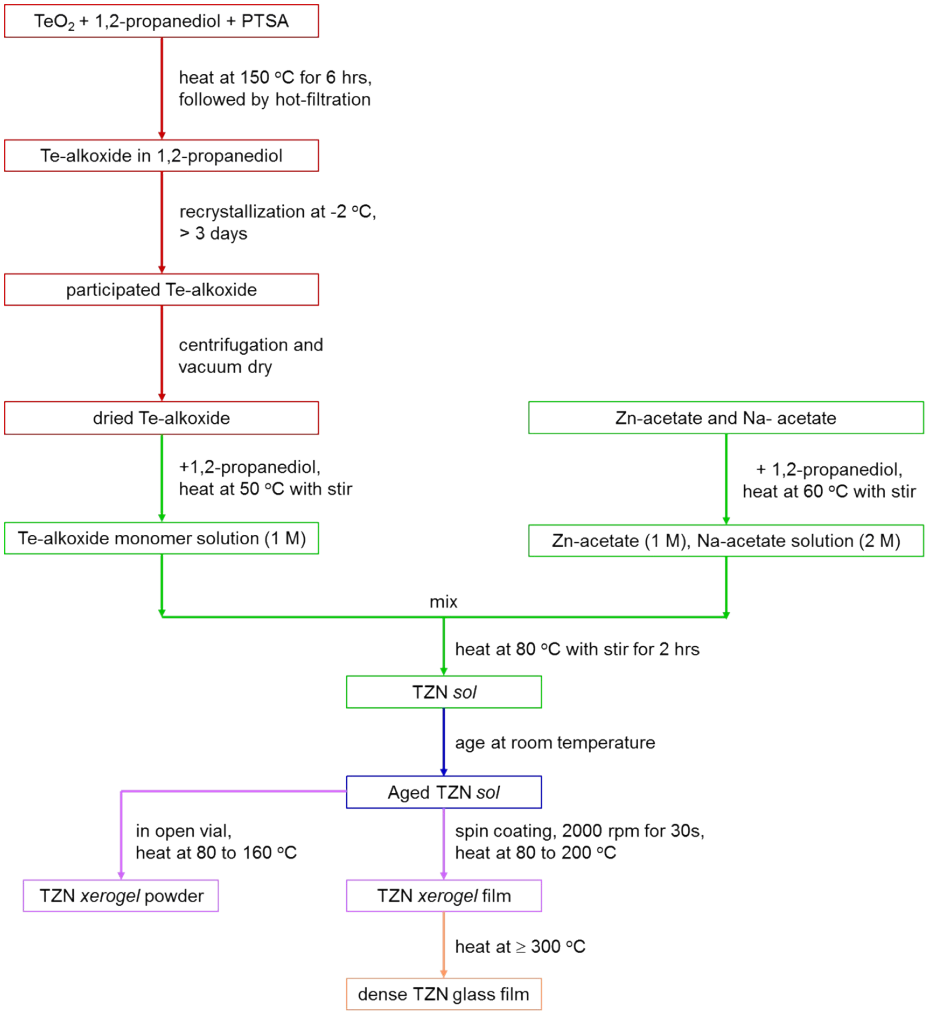

Figure S1. The flow chart shows the synthetic processes in details, where different colors represent the five steps in the whole process: Te-alkoxide (red), TZN *sol* (green), aged TZN *sol* (purple), TZN *xerogel* (pink) and dense TZN glass film (orange).

Preparation of TZN-based glass film in O_2-rich atmosphere: A tube furnace with a glass liner was used to prepare dense-TZN glass films in dry O_2 atmosphere. The film samples were placed in the glass liner at room temperature. Then one end of the liner was connected to the dry O_2 supply and the other end was connected via glass valve to a vacuum pump. (Figure S2a). To remove the air and fill the liner with dry O_2, 4 cycles of vacuuming and O_2 purging were used. After that, the glass valve was disconnected from the vacuum pump and connected to a pipe where part of it is inserted in a flask filled with silicone oil (Figure S2b) to be able to monitor the constant O_2 flow through the glass liner and to prevent backflow of air. The O_2 flow was initially purged at 5 L/min for 30 min to quickly enrich O_2 in the chamber, followed by tuning down to ~0.1 L/min prior to heating up to undertake the *sol*-heating and *xerogel*-heating steps. Such reduced O_2 flow rate is sufficient to replenish and maintain the high O_2 partial pressure, but also to avoid the formation of large temperature gradient across the film sample within the hot zone of the furnace. Under continuous provision of O_2, the placed film samples were then heated as follow: (1) from room temperature to 80/150 °C with a rate of 5 °C/min and dwelled for 12 h; (2) heating to 300 °C with a rate of 1 °C/min and dwelled for 1 h.

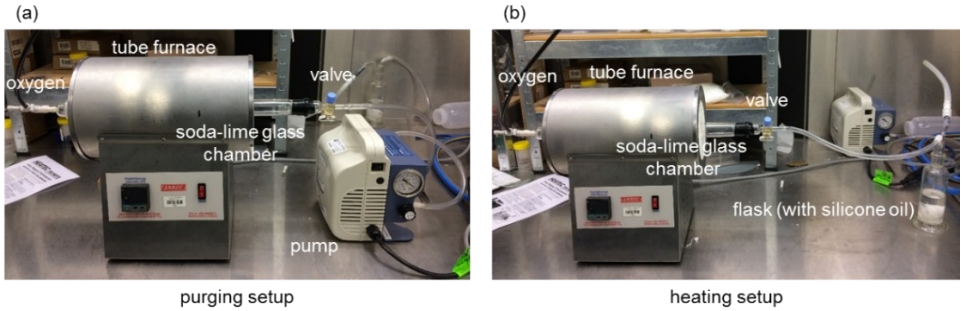

Figure S2. The heating systems used for preparing TZN-based glass films in O_2-rich atmosphere. (a) 4 cycles of vacuuming and O_2 purging to enrich O_2 in the chamber; (b) *sol* heating and *xerogel* heating processes under O_2 flow at ~0.1 L/min which is exhausted via a pipe in a silicone-oil filled flask.

Detailed information for general characterizations

The transmission measurements of TZN glass films on coverslips from 300 nm to 800 nm were performed by using UV-Vis spectrophotometer (Cary 5000, Agilent Technologies), with a scanning speed of 600 nm/min and a step interval of 1 nm. The diameter of the aperture allowing light pass though the samples is 5 mm.

The micro-XRD analysis of the TZN-based films on Si wafers was conducted using a micro-diffractometer (D/MAX-Rapid II Microdiffractometer, Rigaku) with a Cobalt Kα radiation (wavelength 1.7902 Å, accelerating voltage 40 kV, and filament current 15 mA) at a fixed incident angle of 10°. A 0.1 mm collimator, equivalent to an X-ray beam size of approximately 150 × 150 μm, was used for the analysis. Exposure time (on the imaging plate) for each analysis was set to be 10 min. The computer software 2DP was used to convert original 2D imaging data (Debye-Scherrer rings) collected from the curved imaging plate to 1D profiles (i.e. diffraction intensities vs. 2θ), during which, the Si diffraction is eliminated. The powder-XRD analysis of TZN-based powder samples was completed by Rigaku miniflex600 with a copper Kα radiation (wavelength 1.5418 Å, accelerating voltage 40 kV, and filament current 15 mA). The default widths of incident and receiving Soller slits were set to be 2.5°, and the size of divergence slit was selected to be 1.25 °. The widths of scattering slit and receiving slit were all 13 mm. The scanning speed was set at 3° per minute, with a stepping size of 0.02°. The crystalline phases were indexed according to the Rigaku PDXL XRD analysis software and ICDD PDF-2 database.

Thermogravimetric and differential scanning calorimetry (TG-DSC) analysis of TZN *xerogel* powders was performed over the range of 30 to 700 °C by a thermal analysis system (TG-DSC 2 STARe, Mettler Toledo). The TG-DSC curves were acquired with a ramping rate of 10 °C/min under specific atmosphere, i.e. 20% O_2 + 80% N_2 and 80% O_2 + 20% N_2 with flow rate of 3 L/min, respectively. All powder samples were placed in alumina crucibles for TG-DSC analysis. The first derivative of TG data was calculated for differentiate-TG (DTG) curve, which allows to visualize the rate of weight change across the temperature range under consideration.

Simultaneous thermal analysis (STA) was run to monitor the discharged gaseous molecules during heating TZN *xerogels* from 30 to 350 °C, by using hyphenated Fourier transform infrared spectroscopy (vapor-FTIR) (Spectrum 400, Perkin Elmer). The spectra were recorded in the wavenumber range of 500-4000 cm^{-1}, with a resolution of 2 cm^{-1}. The sample chamber was heated at the ramping rate of 5 °C/min and purged with dry air (1.8 L/min).

The molecular weight of Te-alkoxide was identified using mass spectrometry (Bruker, HCT ultra, Germany). Te-alkoxide was dissolved in methanol with a concentration of 0.05 mg/mL, and the resulting solution was subjected to Bruker Daltonik ion-trop MS with a flow rate of 0.1 mL/min. A full scan of the mass range from 220 to 1800 g/mol was acquired by using high capacity spherical traps (HCT) for ionization (by electrospray) of the sample.

An in-house built scanning confocal microscope was used to investigate the optical properties of films, by acquiring the fluorescence intensities distribution of the film in a 2D profile and recording the fluorescent spectra of an arbitrary spot of the film, respectively. The collimated laser beam 532 nm (Crystal Laser, LC-532-100 LO) with a power of 2.56 μW was guided through a 100× magnification objective (Nikon TU Plan Apo, CF 160-2, NA=0.9) and focused onto the film samples. By moving a scanning stage (Piezo XYZ with E-545 PInano@ Piezo controller) with a stepping resolution of 0.3 μm/step, an area of 200 μm × 200 μm is scanned. The fluorescence from film samples was collected by a 2×2 multimode bifurcated fiber (Thorlabs FCMH2-FC), by passing through a 532 nm dichroic beam-splitter (BrightLine@, Di03-R532-t1-25x36) and a 532 nm long-pass filter (RazorEdge@, LP03-532RU-25). These signals were split equally and separately delivered to a photon detector (SPCM, Excelitas Technologies) for imaging acquisition and a spectrometer (iHR320, HORIBA Scienctific) for spectral analysis. The photon counts acquired by photon detector were converted to obtain a 200 μm × 200 μm scanned fluorescence image. The selected spots from the scanned images were pinpointed for fluorescence spectral measurement, recorded by the spectrometer with an exposure time of 30 s.

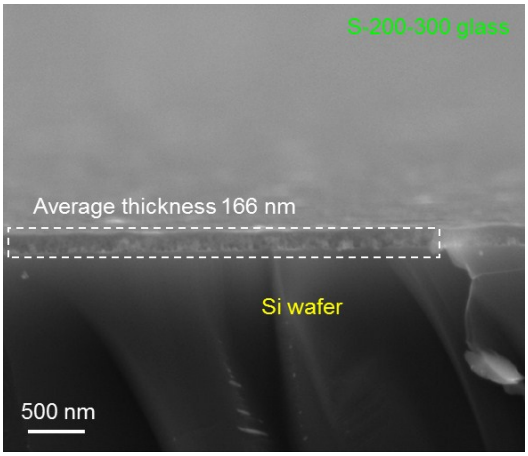

Figure S3. SEM images characterizing the cross-section of a coated film showing its average thickness about 166 nm (S-200-300).

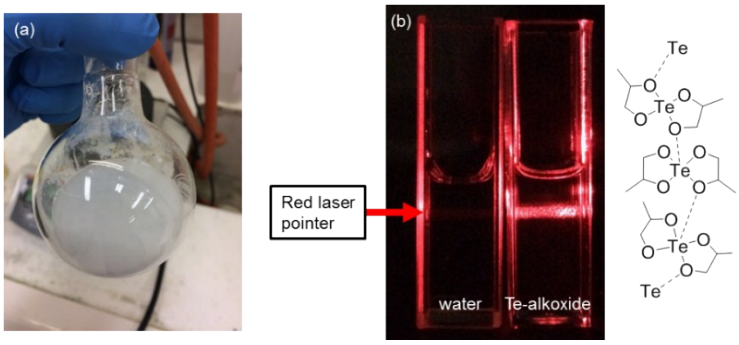

Figure S4. (a) At the stage of preparing Te-alkoxide, the resultant suspension mixture shows the sediment of white powder with interspersed black particles (metallic-Te). (b) The Te-alkoxide molecules linked via weak intermolecular bond (Te···O), showing light scattering under a red laser pointer. The reference water does not appear to such scattering effect.

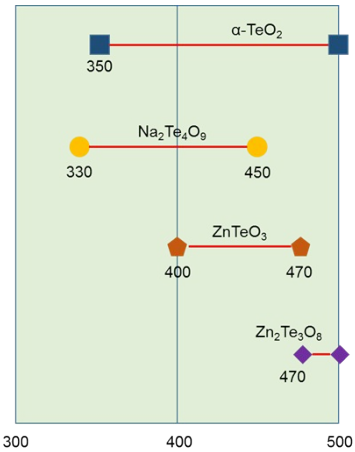

Figure S5. Schematic diagram illustrating the evolution of crystallizations (e.g., α-TeO_2, $Na_2Te_4O_9$, $ZnTeO_3$ and $Zn_2Te_3O_8$ crystals) in TeO_2-based samples from 300 to 500 °C. The data was summarized from references [2-4] and the experimental observation in this work. Note that $Na_2Te_4O_9$ crystal does not appear in our TZN film samples.

Polymerization reactions

As discussed in Section 3.3.2 and 3.3.3 of the main text, the *xerogel* network is formed via both addition and condensation polymerization.

- Schematics illustrating processes of addition polymerization, corresponding to discussion in section 3.3.2, are given below.

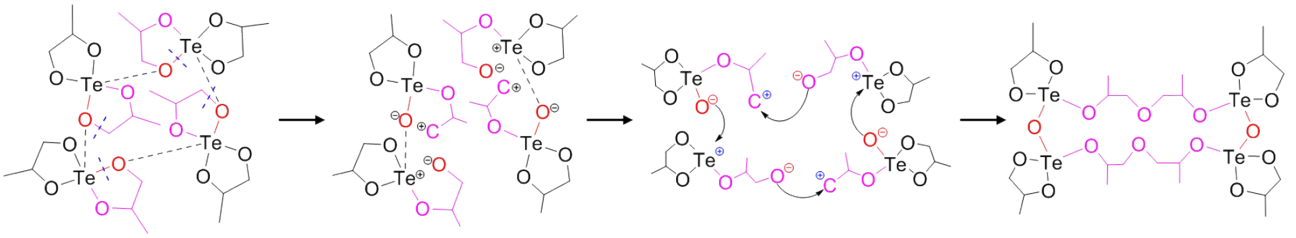

- Schematics illustrating processes of condensation polymerization, corresponding to discussion in section 3.3.2, are given below.

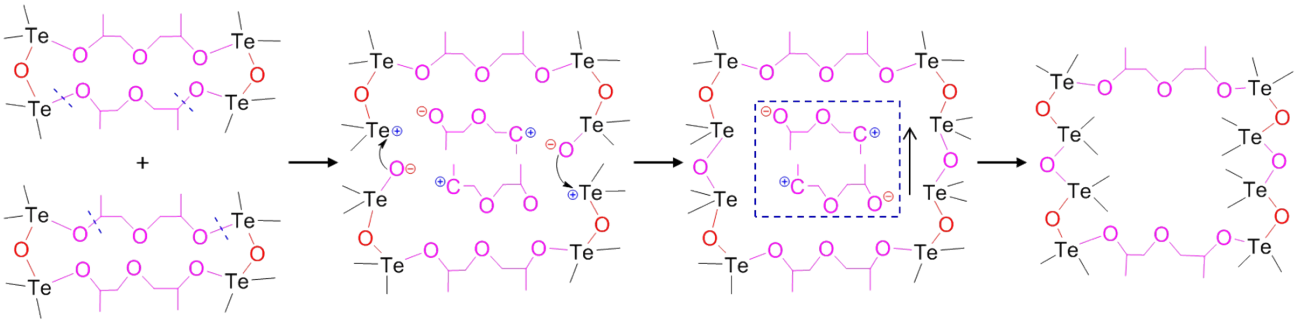

Calculation of the weight ratios of the different types of TeO_4 polyhedra in various *xerogels*

Table S1 summarizes the thermal analysis results (TG-DTG-DSC) of TZN *xerogels*, which were prepared using different aging time (F: 9 days, S: 30-60 days; M: 90 days; L: for 300 days) and different *sol* heating temperature (80, 130 and 150 °C).

sample	region	temp range	DTG peak	DSC peak	Loss *wt%*	Normalized loss *wt%*	comment
Te-alkoxide	I	30-100	none	100 endo	1		no residual solvent/water
F-80	I	30-100	none	105 endo	4		residual solvent/water evaporation
M-80	I	30-100	none		3		residual solvent/water evaporation
L-80	I	30-100	none		1		no residual solvent/water
S-130	I	30-100	none	100 endo	3		residual solvent/water evaporation
F-150	I	30-100	none		0		no residual solvent/water
Te-alkoxide	II	100-250	245	245 endo	97	98	'P' polyhedra evaporation
F-80 *FTIR:*	II	100-250 *160-210*	218	219 endo	74	77	'P' polyhedra evaporation 'Aa' polyhedra decomposition
M-80	II	100-250	193	193 endo	20	21	'Aa' polyhedra decomposition
L-80	II	100-250	205	205 endo	10	10	'Aa' polyhedra decomposition
S-130	II	100-250	170	170 endo	23	24	'Aa' polyhedra decomposition
F-150	II	100-250		238 endo	1	1	'Aa' polyhedra decomposition
Te-alkoxide	III	none			0	0	no combustion
F-80	III	none			0	0	no combustion
M-80	III	250-300	268	273 exo	6	6	'Ao' polyhedral combustion
L-80	III	250-300	262	267 exo	8	8	'Ao' polyhedra combustion
S-130	III	250-300	286	286 exo	4	4	'Ao' polyhedral combustion
F-150 *FTIR:*	III	250-300 *220-300*	268	269 exo	8	8	'Ao' polyhedra combustion

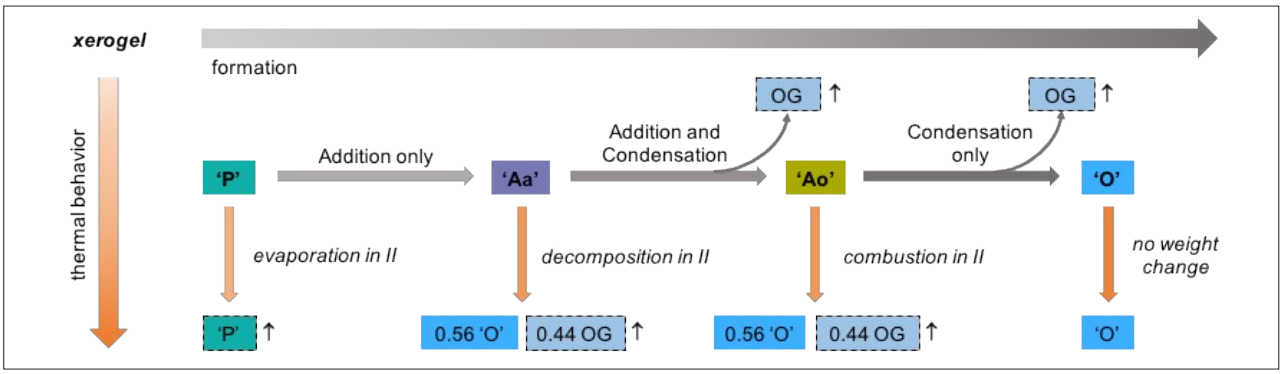

Figure S6. Silver-grey arrow indicating the evolution of [TeO_4] polyhedra of *xerogels* from 'P' polyhedron till 'O' polyhedron, in accompany with the release of OGs when condensation takes place. Orange-yellow arrow showing the respective thermal behavior of the *xerogels* constituting various [TeO_4] polyhedra under different heating temperatures.

Weight loss data normalization (TG):

As shown in the TG-DTG-DSC curves in the main text (section 3.3.1), the weight losses (*wt*%) can be classified into three temperature regions (depicted by the Roman numerals: I, II, III) according to the different DTG peaks, i.e. evaporation of residual solvent in region I; evaporation of P polyhedra and decomposition of Aa polyhedra in region II; combustion of Ao polyhedra in region III.

To determine the weight ratios of the different polyhedra ('P', 'Aa', 'Ao', 'O'), the weight losses measured via TG analysis for region II (L_{II}) and III (L_{III}) are normalized to the total weight (W_{II+III}) in these regions given by $W_{II+III} = L_{II}+L_{III}+R_{III}$, where R_{III} is the weight remains at 300 °C, i.e. $R_{III}=100-L_{I}-L_{II}-L_{II}I$. Accordingly, the normalized weight losses and weight remains in percentage are given by $Y/W_{II+III}\times100\%$, where Y is L_{II}, L_{III} or R_{III}. The normalized values are presented as "normalized loss *wt*%" column in Table S1.

Thermal behavior of polyhedra:

The liberation of all OGs from the molar composition of 80Te-alkoxide–10Zn-acetate–20Na-acetate leads to the $80TeO_2$–$10ZnO$–$10Na_2O$ TZN glass, with a theoretical weight loss of 44% and weight remains of 56%. The detailed calculation is given as below:

The molar mass (g/mol):

Te-alkoxide	Zn-acetate	Na-acetate	TeO2	ZnO	Na2O
278	183	82	162	81	80

Thus the theoretical weight remain portion is:

$$R = 0.8 * \frac{162}{278} + 0.1 * \frac{81}{183} + 0.1 * \frac{80}{2 * 82} = 0.56 = 56\%$$

Thus the weight loss is L=44%.

According to the mass conservation law, the weight of the respective polyhedra (i = 'P', 'Aa', 'Ao', 'O') before the thermal analysis (X_i) is equivalent to the sum of the weight loss (L_i) and weight remains (R_i), i.e. $X_i = L_i + R_i$ measured after thermal analysis. According to the above calculation of weight loss fraction if all OGs are liberated, the ratio of weight loss (L, due to OGs liberation) to weight remains (R) is defined as L/R = 44/56.

As discussed in section 3.3.3, each polyhedron shows different thermal behavior:

- 'P' polyhedra: They are evaporated with no weight remains, i.e. $X_p = L_p$.
- 'Aa' polyhedra: They have a high conformation mobility, and OGs are liberated from the alkoxy bridges via decomposition in region II, with $L_{Aa}/R_{Aa}=44/56$.
- 'Ao' polyhedra: Due to the low conformation mobility, OGs are liberated from the alkoxy bridges via combustion in region III, with $L_{Ao}/R_{Ao}=44/56$.
- 'O' polyhedra: The absence of alkoxy bridges in 'O' polyhedral make them show zero weight loss, i.e. $X_O=R_O$.

Accordingly, a set of equations can be built to calculate the respective weight ratios of the polyhedra:

'P':	$X_P = L_P$,	$R_P=0$,	
'Aa':	$X_{Aa} = 0.44\ X_{Aa} + 0.56\ X_{Aa}$,	$L_{Aa}=0.44\ X_{Aa}$,	$R_{Aa}=0.56\ X_{Aa}$
'Ao':	$X_{Ao} =0.44\ X_{Ao} + 0.56\ X_{Ao}$,	$L_{Ao}=0.44\ X_{Ao}$,	$R_{Ao}=0.56\ X_{Ao}$
'O':	$X_O = R_O$,	$L_O=0$	

Thermal behaviors of xerogels composed of various polyhedra:

The DTG and DSC behavior of the F-80 *xerogel* is highly similar to that of Te-alkoxide crystals (Fig. 4 and Fig. S5). Specifically, an endothermic DSC dip at ~105 °C without DTG peak and an endothermic DSC dip with pronounced DTG peak at ~220 °C in region II have similar position and shape to the respective melting and evaporation peaks of Te-alkoxide crystals (Figure. S5). Furthermore, no weight loss is observed in region III. The total weight loss of 74% over 100-300 °C is larger than the theoretical weight loss of 44%. The similarity to Te-alkoxide precursor crystals and the exceptionally large weight loss indicate the presence of Te-alkoxide precursor molecules (i.e. 'P' polyhedra) in F-80 *xerogel*. The presence of weight remains at 300 °C indicates that the F-80 *xerogel* sample contains other polyhedra than 'P' polyhedra. According to the absence of the combustion DTG peak of region III, F-80 does not contain any 'Ao' polyhedra and hence no 'O' polyhedra. Thus, the weight remains can only be caused by the decomposition of the alkoxy bridges of 'Aa' polyhedra in region II. This allows calculation of the weight ratio of 'Aa' polyhedra from the weight remains. As the weight loss in region II is due to both the evaporation of 'P' polyhedra and the liberation of OGs from 'Aa' polyhedra alkoxy bridge, the weight ratio of 'P' polyhedra is calculated from the region II weight loss and the weight ratio of 'Aa' polyhedra (calculated from the weight remains).

In contrast to F-80, the total weight loss in region II and III of the other *xerogel* samples (M/L-80, S-130, F-150) (Figure. 4b-e) is smaller than the theoretical weight loss of 44%. This suggests that these *xerogels* do not contain precursor molecules (i.e. no 'P' polyhedra) and their OGs have been partially liberated during the longer *sol*-aging time or higher *sol*-heating temperature via condensation reaction, leading to 'Ao' and 'O' polyhedra. The presence of 'Ao' polyhedra agrees with the observation of a combustion DTG peak for all these samples, while the presence of 'Aa' polyhedra is indicated by the decomposition DTG peak. The weight ratios of the 'Aa' and 'Ao' polyhedra is calculated from the measured weight loss in regions II and III corresponding to the liberation of OGs from 'Aa' and 'Ao' polyhedra, respectively. The weight ratio of the 'O' polyhedra is then calculated from the measured weight remains taking into account the weight remains of 'Aa' and 'Ao' polyhedra calculated from their weight ratios.

Based on the above discussion on thermal behaviors of different *xerogels*, we established the equations for the weight ratios of the 4 types of polyhedra in different *xerogels* as follow:

Xerogel	Polyhedra	Equations
F-80	'P'; 'Aa'	$L_{II} = X_p + 0.44\ X_{Aa}$ $R_{III} = 0.56\ X_{Aa}$ $R_{III}=100-L_{II}-L_{III}$
M-80 S-130 L-80 F-150	'Aa', 'Ao', 'O'	$L_{II} = 0.44\ X_{Aa}$ $L_{III} =0.44\ X_{Ao}$ $R_{III} = 0.56\ X_{Aa} + 0.56\ X_{Ao} + 1\ X_O$ $R_{III}=100-L_{II}-L_{III}$

These equations can be readily solved to derive the values of X_{Aa}, X_{Ao} and X_O of different *xerogels* (as given in Table S2), according to the measured weight loss (Table S1 normalized loss *wt*% column) in region II (L_{II}) and region III (L_{III}):

Table S2. The calculated weight ratios of the 'P', 'Aa', 'Ao' and 'O 'polyhedra in different *xerogel*s.

Sample code	'P' polyhedra (%)	'Aa' polyhedra (%)	'Ao' polyhedra (%)	'O' polyhedra (%)
F-80	59	41		
S-130		54	9	37
M-80		47	14	39
L-80		23	18	59
F-150		2	18	80

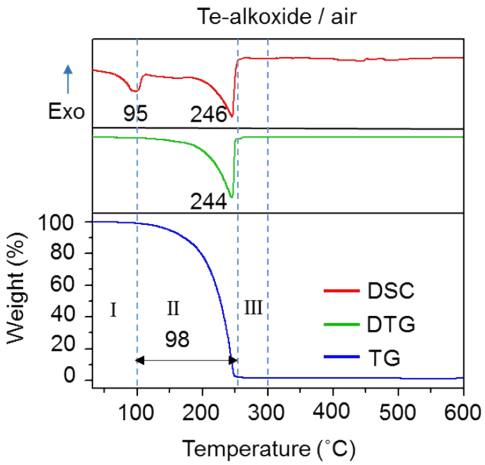

Figure S7. TG-DTG-DSC analysis of as-prepared Te-alkoxide molecules from room temperature to 600 °C with a rate of 10 °C/min under air flow of 3 L/min. Note that the numerical values of DTG and DSC curve indicate the dip temperatures in the regions of I and II. The 95 in DSC corresponds to the melting temperature of Te-alkoxide, while the 246 in DSC and 244 in DTG indicate the evaporation of Te-alkoxide. The number of 98 above the horizontal arrows at the bottom TG curve panel represent *wt*% loss in regions II.

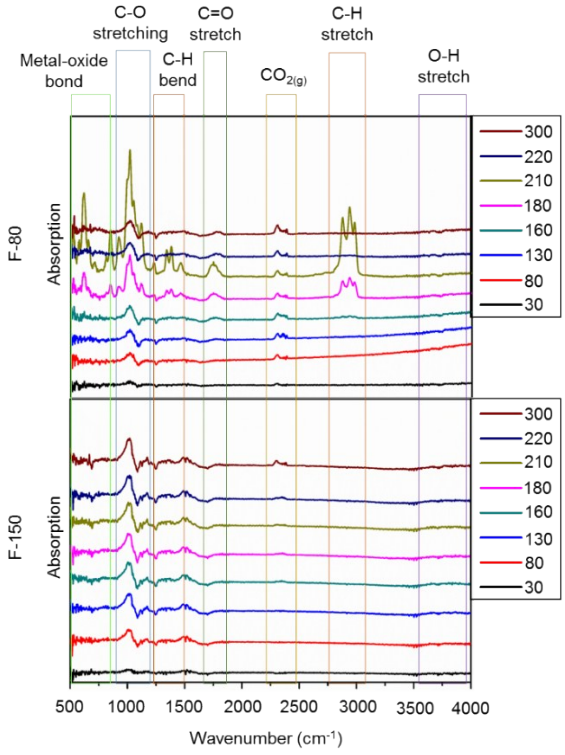

Figure S8. Vapor-FTIR spectroscopic analysis of F-80 and F-150 *xerogels* samples. By heating these samples from 30 to 300 °C in air, the variations of the discharged compounds with different bonds in the vapor were monitored, as indicated by the different color frames.

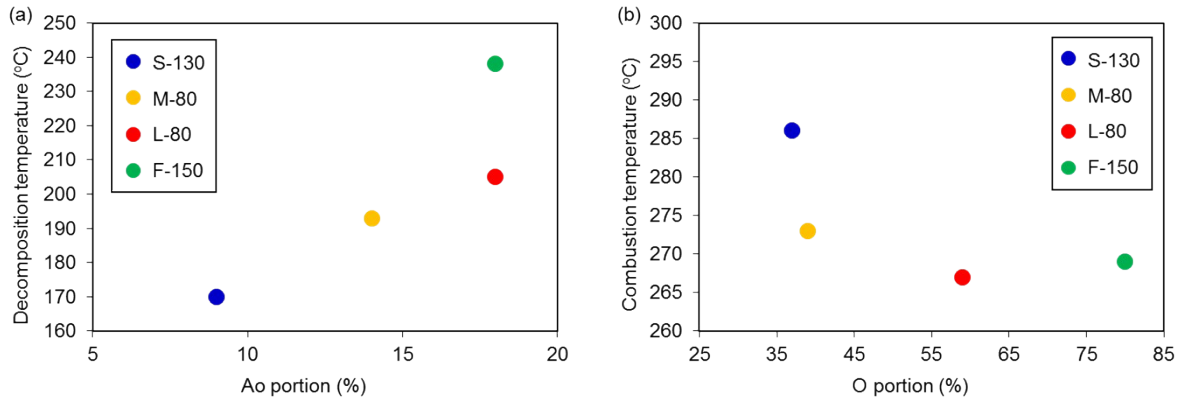

Figure S9. The variations of decomposition and combustion temperatures as a function of the portions of (a) 'Ao' polyhedra and (b) 'O' polyhedra in different *xerogels* samples, respectively. The different color dots indicate various *xerogels*: blue for S-130, yellow for M-80, red for L-80 and organe for F-150. The trend clearly suggests that, in (a), larger portion of 'Ao' polyhedra results in increased decomposition temperature due to the enhanced network around polyhedra, and in (b), increased portion of 'O' polyhedra requires lower combustion temperature due to less organic groups.

Theoretical transmission of 75TeO_2-15ZnO-10Na_2O thin film on coverslip

To determine the theoretical transmission of 75TeO_2-15ZnO-10Na_2O coating on coverslip, the Fresnel reflection at multiple interfaces and the UV-edge absorbance of coverslip were considered.

The refractive index *n* of coverslip (i.e. D 263™ T glass) was simulated according to Sellmeier equation [5]:

$$n^2 = A + B_1\left(\frac{\lambda^2}{\lambda^2 - C_1}\right) + B_2\left(\frac{\lambda^2}{\lambda^2 - C_2}\right) + B_3\left(\frac{\lambda^2}{\lambda^2 - C_3}\right)$$

where A, B_1, B_2, B_3, C_1, C_2 and C_3 are A=1, B_1=1.23795755, B_2=0.0466469, B_3=2.4670056, C_1=0.0086308, C_2=0.0469075, C_3=264.1463 and λ is the wavelength.

The simulated refractive index data of the 75TeO_2-15ZnO-10Na_2O was adopted from Zhao's *et. al.* [6].

The reflection *R* can be calculated via:

$$R = \left(\frac{n_1 - n_2}{n^1 + n^2}\right)^2$$

Thus, the reflection of air/TZN glass interface is:

$$R_1 = \left(\frac{n_g - n_a}{n_g + n_a}\right)^2$$

The reflection of TZN/coverslip interface is:

$$R_2 = \left(\frac{n_g - n_c}{n_g + n_c}\right)^2$$

The reflection of coverslip/air interface is:

$$R_3 = \left(\frac{n_c - n_a}{n_c + n_a}\right)^2$$

where, n_g, n_a, and n_c is the refractive index of TZN glass, air and coverslip, respectively.

The transmission due to the Fresnel reflection taking placing at multiple interfaces is expressed by:

$$T_F = (1 - R_1) * (1 - R_2) * (1 - R_3)$$

The corresponding absorbance caused by this Fresnel reflection is written as:

$$Abs_F = -\log_{10}(T_F)$$

For an uncoated blank coverslip, its absorbance is given as:

$$Abs_C = -\log_{10}(T_C)$$

where $T_C = (1 - R_3)^2$, equivalent to the twice Fresnel reflection at air-coverslip interface.

In addition to Fresnel reflection, the coverslip has a UV-edge absorbance, given by:

$Abs_{C(edge)} = Abs_{C(mes)} - Abs_C$

where $Abs_{C(mes)}$ is the measured Absorbance of coverslip used.

Taking into account the combined contribution by Fresnel reflection of the coated film and the intrinsic absorbance of the coverslip, the theoretical absorbance of $75TeO_2$-$15ZnO$-$10Na_2O$ thin film on coverslip can be calculated as:

$Abs_{TZN\ on\ coverslip} = Abs_{C(edge)} + Abs_F$

As such, the theoretical transmission (%), converted from the theoretical absorbance above, can be written as:

$T_{TZN\ on\ coverslip} = 10^{2 - Abs_{TZN\ on\ coverslip}}$

REFERENCES

1. B. Zheng, M. Zhao, Q. Guo, Y. Yu, S. Lu, X. Jiang and S. Zhou, *J. Mater. Chem. C*, 2015, **3**, 5141-5144.
2. A. Nukui, T. Taniguchi and M. Miyata, *Journal of non-crystalline solids*, 2001, **293**, 255-260.
3. D. W. Lee and K. M. Ok, *Inorganic chemistry*, 2014, **53**, 10642-10648.
4. A. Šantić, A. Moguš-Milanković, K. Furić, M. Rajić-Linarić, C. S. Ray and D. E. Day, *Croatica Chemica Acta*, 2008, **81**, 559-567.
5. SCHOTT, optical glass data sheets, https://refractiveindex.info/download/data/2017/schott_2017-01-20.pdf, 2017).
6. J. Zhao, X. Zheng, E. P. Schartner, P. Ionescu, R. Zhang, T. L. Nguyen, D. Jin and H. Ebendorff-Heidepriem, *Advanced Optical Materials*, 2016, **4**, 1507-1517.